

Active Contours : Recent Developments and a New Rational Approach to Segment Digital Images

Ravinda G.N. Meegama and Jagath C. Rajapakse

School of Computer Engineering, Nanyang Technological University
Nanyang Avenue, Singapore 639798
e-mail: gayan@sentosa.sas.ntu.edu.sg, asjagath@ntu.edu.sg

Abstract

This paper presents recent developments of energy minimizing contour algorithms, or snakes, that are widely used in shape analysis and image processing techniques. The formulae involved in the calculation of energy functions of a closed contour and forces that effect the evolving process of the contour are described. Starting with the discrete model from which snakes were born, we present recently developed snake algorithms, namely, topology adaptive and B-spline snakes. We also propose in this paper a new definition for energy minimizing splines based on Non-Uniform Rational B-Spline (NURBS) curves which allow local shape control by modifying the weights associated with each control point. The results obtained from both synthetic and real images show that snakes with NURBS properties demonstrate more local flexibility than their earlier counterparts.

1 Introduction

The development of snakes was first introduced to the research arena by Kaas, Witkin and Terzopoulos [1]. The model is composed of an elastic curve that changes its shape dynamically to object topologies and is guided by internal forces (elastic forces) and external forces (image and constrained forces), based on local information. The mathematical formulation of the model facilitates integrating image features, desired contour properties and high level knowledge that act as constraint forces to an initial configuration.

The active contour is initialized by drawing an approximate curve around the object of concern. It is then subjected to various forces derived from image features and contour properties that result in the nodes being evolved from one location to another. Algorithmically, snakes are fast, robust, seemingly intelligent and can be subjected to additional restriction forces during the converging process. Robustness to noise and the flexibility to represent a wide variety of shapes have made the snakes generally well-behaved and predictable.

The use of snakes for segmentation and analysis of anatomical structures in the human body and for other image analysis tasks have been investigated by several researchers during the past decades [2, 3, 4, 5]. A majority of these research deals with generalizing the form of the contour and finding better solutions for the convergence and stability problems encountered during energy minimization. However, traditional active contour algorithms, namely, discrete, topological adaptive and B-spline, suffer from the inability to adapt to the topology of the object without increasing the number of snake points. In order to address this issue, we propose a new active contour formulation based on NURBS. The additional weighting term in the NURBS function, unlike its predecessors, influences the snake to attract towards the control points without adding new control points.

2 The Snakes Model

Definition 1. Image: An image is defined as a function $I : \Omega \rightarrow Q$ in which $I(\mathbf{p})$ gives the intensity at the pixel location $\mathbf{p} \in \Omega$ where $\Omega \in \mathbb{N}^2$ is the 2D image domain. The value $Q = \{0, 1, \dots, 255\}$ denotes the set of intensity levels that a pixel location can take.

Definition 2. Curve. A curve is a one parameter vector-valued mathematical function $\mathbf{v} : [0, 1] \rightarrow \Omega$ such that an arbitrary point on the curve \mathbf{v} is parametrically expressed as $\mathbf{v}(s) = (x(s), y(s))$, $s \in [0, 1]$.

Definition 3. Internal Energy: The internal energy E_{int} at a point $\mathbf{v}(s)$ on a curve \mathbf{v} defines the amount of stretching and bending the curve can undergo and is given by

$$E_{int}(\mathbf{v}(s)) = \frac{1}{2} \left(\alpha \left| \frac{\partial \mathbf{v}(s)}{\partial s} \right|^2 + \beta \left| \frac{\partial^2 \mathbf{v}(s)}{\partial s^2} \right|^2 \right) \quad (1)$$

where the constants $\alpha, \beta \in \mathbb{R}$ spell the amount of stretching and flexing on the contour, respectively.

Large values of α increase the internal energy of the curve as it stretches widely while small values make the energy function insensitive to the amount of stretch. Similarly, large values of β increase the internal energy as it forms more curve segments with large curvatures while small values of β make the internal energy function insensitive to curves.

Definition 4. External Energy: The external energy E_{ext} at a point $\mathbf{v}(s)$ on a curve \mathbf{v} is determined by the intensity features of an image such that

$$E_{ext}(\mathbf{v}(s)) = -\frac{1}{2}\gamma |\nabla I(\mathbf{v}(s))|^2 \quad (2)$$

where $\gamma \in \mathbb{R}$ is called the the edge coefficient.

Large positive values of γ tend to make the curve align itself with dark regions on the image I whereas large negative values of γ make it align itself with bright regions.

Definition 5. Balloon Energy: The balloon energy E_{bal} on a curve point $\mathbf{v}(s)$ is defined as

$$E_{bal}(\mathbf{v}(s)) = \delta \left(1 - \frac{|\nabla I(\mathbf{v}(s))|^2}{\|\nabla I(\mathbf{v}(s))\|^2} \right) \quad (3)$$

where $\delta \in \mathbb{R}$ is the amplitude of the balloon force [6].

The balloon energy ensures that the curve is not attracted towards weak edges or spurious noise and makes it inflate near high intensity regions and deflate at low intensity areas according to region-based image intensity statistics [7].

The total energy E of the curve \mathbf{v} can now be represented as an integral of internal, external and balloon energies as follows:

$$E(\mathbf{v}) = \int_0^1 (E_{int}(\mathbf{v}(s)) + E_{ext}(\mathbf{v}(s)) + E_{bal}(\mathbf{v}(s))) ds \quad (4)$$

Definition 6. Dynamic Curve: A dynamic curve is a two parameter vector-valued mathematical function $\mathbf{v} : [0, 1] \times [0, \infty) \rightarrow \Omega$ defined in terms of its x and y coordinates which in turn are parameterized by a linear parameter $s \in [0, 1]$ and time $t \in [0, \infty)$ such that $\mathbf{v}(s, t) = (x(s, t), y(s, t))$.

Definition 7. Active contour: An active contour is a dynamic curve that evolves over time trying to minimize its total energy such that if $\mathbf{v}(t)$ represents a contour at time t , the curve at time $t + 1$ can be found by

$$\mathbf{v}(t + 1) = \arg \min_{\mathbf{v} \in \mathcal{V}} E(\mathbf{v}(t))$$

where \mathcal{V} is the set of all possible dynamic contours and $E(\mathbf{v}(t))$ is the total energy of the contour \mathbf{v} at time t .

3 Snake Algorithms

The major active contour models that have been developed and widely used in recent research literature are presented in the following.

3.1 Discrete Snakes

A *discrete snake* was first used to introduce the principles of energy minimizing contours in [1]. It is an active contour that maintains a constant number of nodes around its closed curve segment until energy minimization is achieved. Although it is easy to implement, the accuracy of the final result is limited to the fact that the number of nodes does not increase when the snake expands.

A discrete representation for the expressions in the right hand side of eq. (1) could be given in finite differences as

$$\frac{\partial \mathbf{v}_i}{\partial s} = \frac{|\mathbf{v}_i - \mathbf{v}_{i-1}|}{\max_j \{\mathbf{v}_j - \mathbf{v}_{j-1}\}}$$

and

$$\frac{\partial^2 \mathbf{v}_i}{\partial s^2} = \frac{|\mathbf{v}_{i+1} - 2\mathbf{v}_i + \mathbf{v}_{i-1}|}{\max_j \{\mathbf{v}_{j+1} - 2\mathbf{v}_j + \mathbf{v}_{j-1}\}}$$

where \mathbf{v}_i , $i = 0, \dots, n - 1$ are the n discrete pixel locations that form the active contour. The algorithm for evolving a discrete snake is as follows:

```

Initialize  $\alpha$ ,  $\beta$ ,  $\gamma$  and  $\delta$ 
Initialize snake nodes
 $\lambda$  = number of iterations
 $i = 0$ 
 $n$  = number of snake nodes
Repeat {
  For  $j = 0$  to  $n - 1$  {
    Computer energy at node  $\mathbf{v}_j$ 
    Move  $\mathbf{v}_j$  to minimal energy location
  }
   $i = i + 1$ 
}Until (snake converged or  $i = \lambda$ )

```

3.2 Topology Adaptive Snakes

A discrete snake has a major drawback in that it cannot penetrate into regions with high curvatures for the lack of nodes. One such basic method that solves this problem is to take the distance between two consecutive nodes and add or delete nodes based on this distance. This has the ability to increase or decrease the number of nodes in order to converge into high curvature regions by increasing the number of nodes in the contour giving an accurate segmentation.

Let d_i be the Euclidean distance between the snake nodes \mathbf{v}_i and \mathbf{v}_{i-1} . Also let T_d and T_k be the average Euclidean distance between the nodes and

the average curvature of the snake. The curvature κ_i of the snake at a node \mathbf{v}_i is found using the second derivative of $\mathbf{v}_i(s)$ with respect to s such that $\kappa_i = \frac{\partial^2 \mathbf{v}_i}{\partial s^2}$. The relevant finite difference formulae is given in section 3.1. Then, a pseudo code to represent the evolution is given as follows:

```

Initialize  $\alpha, \beta, \gamma$  and  $\delta$ 
Initialize snake nodes
 $c = 0$ 
 $n =$  number of snake nodes
Repeat {
  For  $i = 0$  to  $n - 1$  {
    If ( $d_i \geq T_d$ ) and ( $\mathcal{K}_i \geq T_k$ )
      add node between  $\mathbf{v}_{i+1}$  and  $\mathbf{v}_i$ 
    elseif ( $d_i \geq T_d$ ) and ( $\mathcal{K}_i < T_k$ )
      remove  $\mathbf{v}_i$ 
    else no change to number of nodes
  }
   $n =$  updated number of snakes nodes
  For  $j = 0$  to  $n - 1$  {
    Computer energy at node  $\mathbf{v}_j$ 
    Move  $\mathbf{v}_j$  to minimal energy location
  }
   $c = c + 1$ 
}Until (snake converged or  $c = \lambda$ )

```

Another efficient method that introduces topological flexibility for active contours is introduced in [8]. It spells out a re-parameterization method for the contour at each iteration step using an affine cell decomposition technique. The image space is subdivided into a grid of cells. At each deformation step, the cell vertices that the snake roll over are marked. The set of vertices that reside inside the T-snake is taken as the boundary of the model.

4 B-spline Snakes

The type of snakes that are presented in the previous section suffer from the limitation in that the movement of a single snake node affects the entire length of the contour which is described as *global propagation* of change of a particular node. The advantage of B-spline active contours is that the evolution of a snake point affects only the local contour segment to which that point belongs [9]. It uses a set of blending functions having only local influence and depends only on the immediate neighboring control points. Further, in B-spline snakes, the degree of the curve function is independent of the number of control points [10].

Let $\mathbf{p}_i, i = 0, 1, \dots, n - 1$ be the control points of a B-spline curve \mathbf{v} of degree $k \in \mathbb{Z}^+$ that is given by

$$\mathbf{v}(s) = \sum_{i=0}^{n-1} N_{i,k}(s) \mathbf{p}_i \quad (5)$$

where $N_{i,k}$ is the B-spline basis function of degree k such that

$$N_{i,0}(s) = \begin{cases} 1, & \text{if } s_i \leq s < s_{i+1} \\ 0, & \text{otherwise.} \end{cases}$$

$$N_{i,k}(s) = \frac{(s - s_i)N_{i,k-1}(s)}{s_{i+k-1} - s_i} + \frac{(s_{i+k} - s)N_{i+1,k-1}(s)}{s_{i+k} - s_{i+1}}$$

in which $(s_0, s_1, \dots, s_{n+k+1})^T$ is the *knot vector*.

The B-spline contour given in (5) is defined in the vector form as

$$\mathbf{v} = \mathbf{p}^T \mathbf{N}$$

where $\mathbf{p} = (\mathbf{p}_0, \mathbf{p}_1, \dots, \mathbf{p}_{n-1})^T$ and $\mathbf{N} = (N_{0,k}, N_{1,k}, \dots, N_{n-1,k})^T$.

The internal energy of a B-spline snake node $\mathbf{v}(s)$ is defined as

$$E_{int}(\mathbf{v}(s)) = \frac{1}{2} \{ \alpha \mathbf{p}^T \mathbf{N}' + \beta \mathbf{p}^T \mathbf{N}'' \}$$

where

$$\frac{\partial \mathbf{N}}{\partial s} = \mathbf{N}' = (N'_{0,k}, N'_{1,k}, \dots, N'_{n-1,k})^T$$

Let $\mathbf{p}_i = (x_i, y_i)^T$. Then, eq. (5) is written as

$$\mathbf{v}(s) = \sum_{i=0}^{n-1} N_{i,k}(s) (x_i, y_i)$$

Now, any point on the snake is expressed as $\mathbf{v}(s) = (x(s), y(s))$ where $x(s) = \sum_i N_{i,k}(s) x_i$ and $y(s) = \sum_i N_{i,k}(s) y_i$. If $\mathbf{x} = (x_0, x_1, \dots, x_{n-1})^T$ and $\mathbf{y} = (y_0, y_1, \dots, y_{n-1})^T$, the external energy at a point $(x(s), y(s))$ is written as

$$E_{ext}((x(s), y(s))) = -\frac{1}{2} \gamma |\nabla I(\mathbf{x}^T \mathbf{N}, \mathbf{y}^T \mathbf{N})|^2 \quad (6)$$

and also the balloon energy as

$$E_{bal}(x(s), y(s)) = \delta \left(1 - \frac{|\nabla I(\mathbf{x}^T \mathbf{N}, \mathbf{y}^T \mathbf{N})|^2}{\|\nabla I(\mathbf{x}^T \mathbf{N}, \mathbf{y}^T \mathbf{N})\|^2} \right)$$

5 NURBS Snakes

In B-spline snakes, in order to increase the flexibility, new control points must be added thereby, increasing computational times. To overcome this problem, a new formulation for active contour models based on NURBS is proposed in this section (a

complete description of NURBS, their properties and advantages can be found in [11]).

A NURBS curve $\mathbf{v}(s)$ of degree k is defined as a two parameter vector-valued rational functional as follows

$$\mathbf{v}(s) = \frac{\sum_{i=0}^{n-1} w_i N_i(s) \mathbf{p}_i}{\sum_{i=0}^{n-1} w_i N_i(s)}$$

where $w_i \in \mathbb{R}^+$ are the weights and $N_{i,k}$ are the B-spline basis functions as defined in the previous section. It is also written as

$$\mathbf{v}(s) = \sum_{i=0}^{n-1} R_{i,k}(s) \mathbf{p}_i$$

where $R_{i,k}$ is the rational basis functions of degree k such that

$$R_{i,k}(s) = \frac{w_i N_{i,k}(s)}{\sum_{j=0}^{n-1} w_j N_{j,k}(s)}$$

It can be further derived that

$$\frac{\partial R_{i,k}(s)}{\partial s} = \frac{w_i \{Q N'_{i,k}(s) - N_{i,k}(s) Q'\}}{Q^2}$$

and

$$\frac{\partial R_{i,k}^2(s)}{\partial s^2} = \frac{Q w_i \{Q N''_{i,k}(s) - N_{i,k}(s) Q''\} - 2Q' w_i \{Q N'_{i,k}(s) + Q' N_{i,k}(s)\}}{Q^3}$$

where $Q = \mathbf{w}^T \mathbf{N} \neq 0$ and $\mathbf{w} = (w_0, w_1, \dots, w_{n-1})^T$.

Then, the internal energy of the snake node $\mathbf{v}(s)$ is

$$E_{int}(\mathbf{v}(s)) = \frac{1}{2} \left\{ \alpha |\mathbf{p}^T \mathbf{R}'|^2 + \beta |\mathbf{p}^T \mathbf{R}''|^2 \right\}$$

where $\mathbf{R} = (R_{0,k}, R_{1,k}, \dots, R_{n-1,k})^T$.

An arbitrary point $(x(s), y(s))$ on the NURBS snake can be expressed as $x(s) = \sum_i R_{i,k}(s) x_i$ and $y(s) = \sum_i R_{i,k}(s) y_i$. By using a similar expression as given in eq. (6), the external energy of the NURBS snake at a point $(x(s), y(s))$ is given by

$$E_{ext}(x(s), y(s)) = -\frac{1}{2} \gamma |\nabla I(\mathbf{x}^T \mathbf{R}, \mathbf{y}^T \mathbf{R})|^2$$

and also the balloon energy by

$$E_{bal}(x(s), y(s)) = \delta \left(1 - \frac{|\nabla I(\mathbf{x}^T \mathbf{R}, \mathbf{y}^T \mathbf{R})|^2}{\|\nabla I(\mathbf{x}^T \mathbf{R}, \mathbf{y}^T \mathbf{R})\|^2} \right)$$

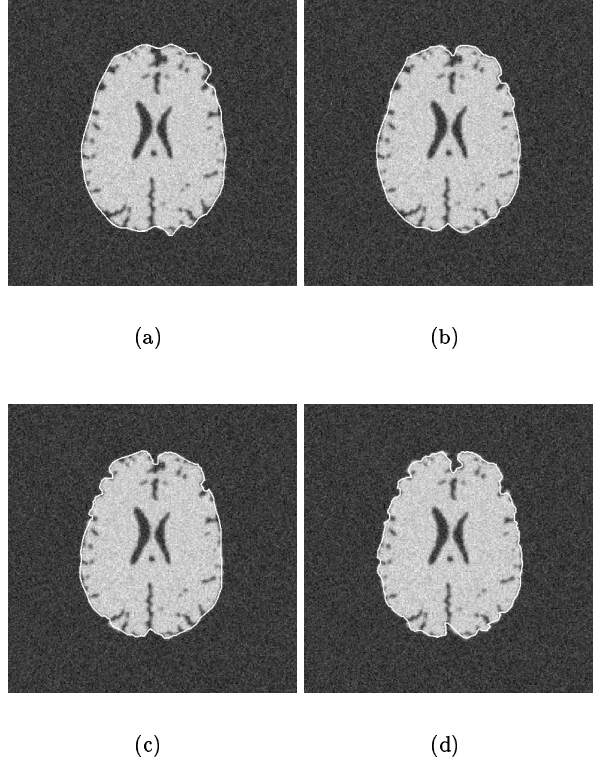


Figure 1: Snakes models converged on synthetic images: (a) discrete snake, (b) topological adaptive snakes, (c) B-spline snakes and (d) NURBS snakes

Eventhough the NURBS-based active contour that we propose inherits the properties of B-spline snakes, the most important feature in this model is the inclusion of a weighting parameter to each control point which allows local shape control without adding new control points. Whenever the curvature κ_i^{t+1} at a control point \mathbf{p}_i^{t+1} at time $t+1$ exceeds the average curvature, the weight w_i^{t+1} at the control point \mathbf{p}_i^{t+1} is computed as

$$w_i^{t+1} = w_i^t + \eta \frac{\kappa_i^{t+1}}{\max_i \{\kappa_i^{t+1}\}}$$

where $\eta \in \mathbb{R}$. Hence, the higher the curvature at a particular point, the greater the attraction of the curve towards that control point.

NURBS-based deformable models, called D-NURBS (Dynamic NURBS), for computer aided geometric design was investigated in [12]. It is an interactive environment where the user can sculpt complex shapes by applying simulated forces together with local and global shape constraints. In this technique, the weights near the desired regions have to be interactively adjusted by the designer in order to influence the shape of the curve.

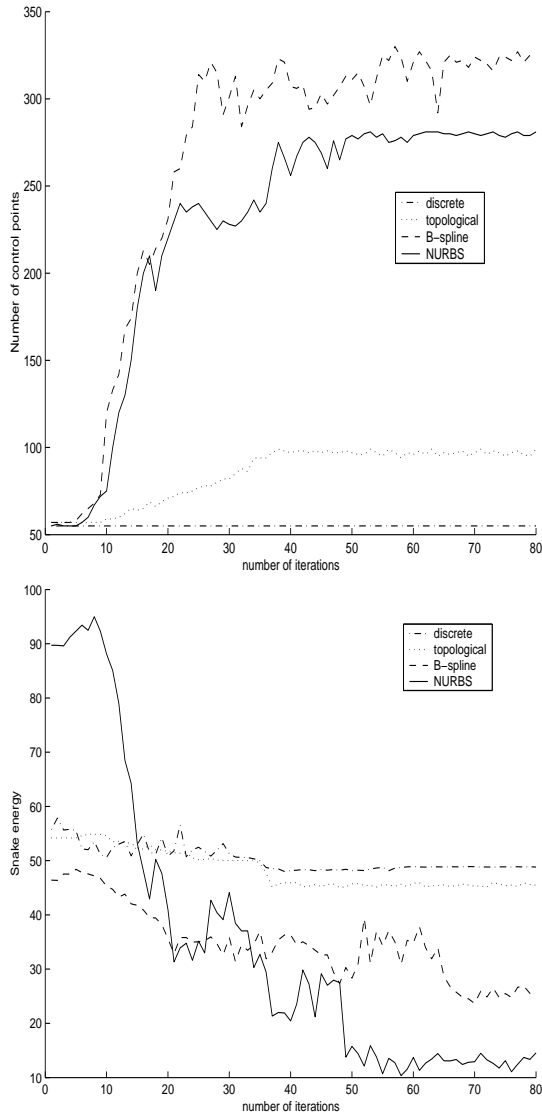


Figure 2: Graphs showing (top) the change of number of nodes and (bottom) energy minimization of the snake models when applied on the synthetic image.

6 Experimental Results

In order to obtain a measure for the snake model that extracts the most accurate boundary of the brain matter, we make use of the *similarity index (SI)* proposed in [13]. This method has also been used in a similar study to quantify segmentation results obtained from active contours [2]. To calculate *SI*, which is sensitive to both the size and the location of the active contour, the actual boundary is extracted by manually outlining the outer boundary of the concerned object in the image.

snake models	<i>SI</i>
discrete	0.956
topological adaptive	0.971
B-spline	0.979
NURBS	0.995

Table 1: Comparison of areas enclosed by the actual boundary and the snake contours in synthetic images.

6.1 Experiments with Synthetic Images

The convergence of the snake models on a synthetic image is illustrated in Figure 1. This 256×256 image consisted of a signal-to-noise ratio (SNR) of 10 dB. We have analyzed the convergence process by using the graphs shown in the Figures 2. It is seen that the energy minimization was achieved best with the NURBS snakes eventhough it consisted of relatively lesser number of distinct points than the B-spline snake.

The values of *SI* are shown in Table 1 for the four snake models. The NURBS snake model gives the highest value for *SI*. In other words, this model managed to converge to the nearest actual boundary of the object of interest compared with the other three.

6.2 Experiments with Digital Images

The versatility and the flexibility of the proposed NURBS snakes were further tested on clinical images, acquired by a digital camera, to detect the area of a *melanoma*; a skin lesion that arises in the cells producing pigments [14]. Measuring the physical dimensions of such a skin disease is important for a pathologist to track the spread of the infection and record the progress of healing. The area of the lesion, shown in Figure 3, was manually measured to be 26638 square pixels. It is clear from the values given in Table 2 that the NURBS snakes captured the boundary of the lesion with a higher precision than the other snake models.

7 Conclusion

In this paper, we have presented a mathematical formulation for a new type of snake model based on NURBS. It is also a model driven approach where each individual snake node has greater flexibility and independency from its neighbors. Moreover, NURBS-based snakes allow insertion of additional control points dynamically during the evolution stages without increasing the degree of the curve. The additional weighting parameter facilitates attracting the snake towards the control points when

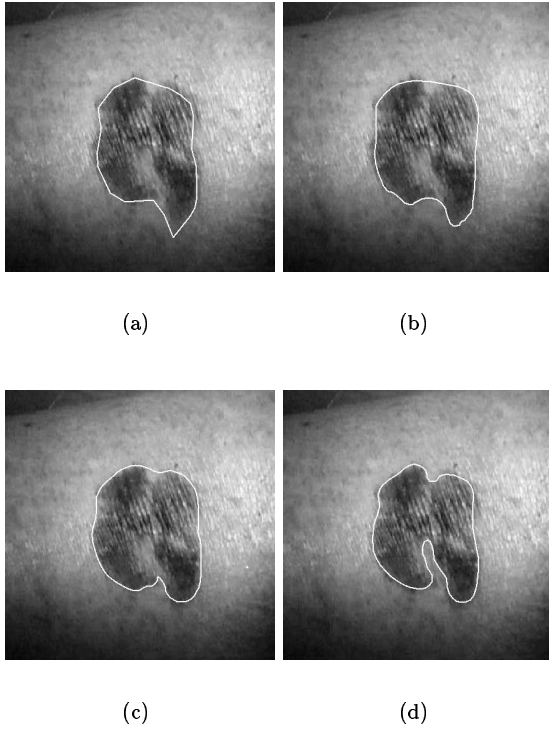


Figure 3: Snake models converged on a digital image: (a) discrete, (b) topological adaptive, (c) B-spline snake and (d) NURBS snake.

snake models	SI
discrete	0.907
topological adaptive	0.925
B-spline	0.941
NURBS	0.997

Table 2: Comparison of areas enclosed by the actual boundary and the snake contours in real images.

the curvature is high without increasing the number of control points.

References

- [1] M. Kaas, A. Witkin, and D. Terzopoulos, "Snakes: Active contour models," *Int. Journal of Computer Vision*, vol. 1, no. 4, pp. 321–331, 1988.
- [2] S. Atkins and B. Mackiewicz, "Fully automated segmentation of the brain in MRI," *IEEE Trans. Medical Imaging*, vol. 17, no. 1, pp. 99–107, 1998.
- [3] C.A. Davatzikos and J.L Prince, "An active contour model for mapping the cortex," *IEEE Trans. Medical Imaging*, vol. 14, no. 1, pp. 65–80, 1995.
- [4] T. McInerny and D. Terzopoulos, "Deformable models in medical image analysis," in *Proc. Workshop on Mathematical Methods in Biomedical Image Analysis*, pp. 171–180, 1996.
- [5] S. Menet, P.S. Marc, and G. Medioni, "Active contour models: Overview, implementation and applications," in *Proc. IEEE Int. Conf. Systems, Man and Cybernatics*, pp. 194–199, 1990.
- [6] L.D. Cohen, "On active contour models and balloons," *CVGIP: Image Understanding*, vol. 53, no. 2, pp. 211–218, 1991.
- [7] T. McInerny and D. Terzopoulos, "Topology adaptive deformable surface for medical image volume segmentation," *IEEE Trans. Medical Imaging*, vol. 18, no. 10, pp. 840–850, 1999.
- [8] T. McInerny and D. Terzopoulos, "T-snakes: Topology adaptive snakes," *5th ICCV*, pp. 840–845, 1995.
- [9] M. Flickner, H. Sawbrey, D. Pryor, and J. Lotspiech, "Interactive image outlining using B-spline snakes," *28th Asilomar Conf. Signals, Systems and Computers*, vol. 1, pp. 731–735, 1994.
- [10] M.E. Mortenson, *Geometric Modeling*, John-Wiley, New York, 1985.
- [11] L. Piegl and W. Tiller, *The NURBS Book*, Springer-Verlag, 1995.
- [12] H. Qin and D. Terzopoulos, "D-NURBS: A physics-based framework for geometric design," *IEEE Trans. Visualization and Computer Graphics*, vol. 2, no. 1, pp. 85–95, 1996.
- [13] A.P. Zijdenbos, B.M. Davant, R.A. Margolin, and A.C. Palmer, "Morphometric analysis of white matter lesions in MR images: Methods and validation," *IEEE Trans. Medical Imaging*, vol. 13, no. 4, pp. 716–724, 1994.
- [14] M. Brygel, *Video Book of Surgery*, North-East Valley Division of General Practice, Victoria, Australia, 2000.